Specific Bacterial, Archaeal, and Eukaryotic Communities in Tidal-Flat Sediments along a Vertical Profile of Several Meters

Reinhard Wilms, Henrik Sass, Beate Köpke, Jürgen Köster, Heribert Cypionka and Bert Engelen

Appl. Environ. Microbiol. **2006, 72(4):2756. DOI: 10.1128/AEM.72.4.2756-2764.2006.**

Applied and Environmental Microbiology, Apr. 2006, p. 2756–2764 Vol. 72, No. 4
0099-2240/06/$08.00+0 doi:10.1128/AEM.72.4.2756–2764.2006

Specific Bacterial, Archaeal, and Eukaryotic Communities in Tidal-Flat Sediments along a Vertical Profile of Several Meters†

Reinhard Wilms, Henrik Sass,‡ Beate Köpke, Jürgen Köster, Heribert Cypionka, and Bert Engelen*

Institut für Chemie und Biologie des Meeres, Carl-von-Ossietzky Universität Oldenburg, Carl-von-Ossietzky Straße 9-11, D-26129 Oldenburg, Germany

Received 8 December 2005/Accepted 13 February 2006

The subsurface of a tidal-flat sediment was analyzed down to 360 cm in depth by molecular and geochemical methods. A community structure analysis of all three domains of life was performed using domain-specific PCR followed by denaturing gradient gel electrophoresis analysis and sequencing of characteristic bands. The sediment column comprised horizons easily distinguishable by lithology that were deposited in intertidal and salt marsh environments. The pore water profile was characterized by a subsurface sulfate peak at a depth of about 250 cm. Methane and sulfate profiles were opposed, showing increased methane concentrations in the sulfate-free layers. The availability of organic carbon appeared to have the most pronounced effect on the bacterial community composition in deeper sediment layers. In general, the bacterial community was dominated by fermenters and syntrophic bacteria. The depth distribution of methanogenic archaea correlated with the sulfate profile and could be explained by electron donor competition with sulfate-reducing bacteria. Sequences affiliated with the typically hydrogenotrophic *Methanomicrobiales* were present in sulfate-free layers. Archaea belonging to the *Methanosarcinales* that utilize noncompetitive substrates were found along the entire anoxic-sediment column. Primers targeting the eukaryotic 18S rRNA gene revealed the presence of a subset of archaeal sequences in the deeper part of the sediment cores. The phylogenetic distance to other archaeal sequences indicates that these organisms represent a new phylogenetic group, proposed as "tidal-flat cluster 1." Eukarya were still detectable at 360 cm, even though their diversity decreased with depth. Most of the eukaryotic sequences were distantly related to those of grazers and deposit feeders.

It has been estimated, that marine subsurface habitats harbor the majority of the global prokaryotic biomass (55). Despite the inhospitality of subsurface sites, remarkably diverse microbial communities were found within the deep biosphere tens to hundreds of meters below the seafloor (15, 31). Microbiological investigations on marine subsurface communities mainly focused on the deep biosphere in open-ocean and continental-margin sediments (8, 34). So far, little attention has been paid to the subsurface of coastal sediments (49), but the number of publications is increasing (23, 29, 56).

Tidal flats are characterized by high primary production rates and consequently intense remineralization in the sediment (10, 38, 39). Furthermore, they exhibit high sedimentation rates and, in contrast to open-ocean sites (8, 35), steep chemical gradients, with oxygen generally being depleted within a few millimeters below the sediment surface (2). Nevertheless, tidal-flat sediments show a strong patchiness as oxic microniches can be found down to a depth of 20 cm along the burrows of the zoobenthos (40). In layers beneath, however, microbial processes are strictly anaerobic and seem to be governed by the sequence of electron acceptors along the redox series, with sulfate appearing to be the most important one.

Erosion of the upper sediment layers by storm-driven currents and changes in flat topography by tidal creeks often lead to the formation of contrasting depositional areas. These are characterized by sediments of different grain sizes, even in close proximity. Over time, the patchiness together with the influence of burrowing macrozoobenthos (40) results in a three-dimensional mosaic of microenvironments. Therefore, the question arises of whether geochemical profiles are stable and how the microbial-community composition is influenced.

Previous microbiological studies on tidal flats analyzed the supposedly most active uppermost 50 cm and focused mostly on bacterial communities (21, 25, 30). The first insights into the bacterial-community composition of deeper tidal-flat sediments via a cultivation-based approach revealed a shift from predominance by *Proteobacteria* to that of *Firmicutes* with depth (23). A comparison of bacterial communities at three sedimentologically distinct sites on the same sampling location was performed by a molecular approach. For the deepest layers the community composition showed similarities to those of deep subsurface sites (56). Investigations on archaeal communities in tidal flats are still rare (20), even though high abundance and diversity of archaea were found in marine subsurface sediments (5, 17). Eukaryotic communities within these habitats have been even less investigated, and only recently they became a subject of molecular studies (14, 28).

The present study, however, aims to fill a gap between the different studies by analyzing bacterial, archaeal, and eukary-

* Corresponding author. Mailing address: Institut für Chemie und Biologie des Meeres, AG Paläomikrobiologie, Universität Oldenburg, Postfach 2503, D-26111 Oldenburg, Germany. Phone: 49-441-798-5376. Fax: 49-441-798-3585. E-mail: engelen@icbm.de.

† Supplemental material for this article may be found at http://aem.asm.org/.

‡ Present address: School of Earth, Ocean and Planetary Sciences, Cardiff University, Main Building, Park Place, Cardiff CF10 3YE, Wales, United Kingdom.

otic communities on one site as well as by comparing subsurface with surface layers and correlating community composition with sedimentological and geochemical parameters.

MATERIALS AND METHODS

Sample collection. Sediment cores were collected from a back-barrier tidal-flat area close to the island of Spiekeroog, Germany (53°43.270′N, 7°43.718′E), in June 2002 (core A), October 2003 (core B), February 2004 (core C), and September 2005 (core D). Aluminum tubes with a diameter of 8 cm were driven into the sediment by the use of a vibration unit (vibrocoring) and were recovered by using a lifting block. During each sampling campaign, single cores were taken and processed. Surface samples were taken separately. The tubes of cores A to C were cut longitudinally and prized open to obtain a uncontaminated surface for subsampling, whereas core D was sectioned transversely to avoid degassing of methane during sampling. Samples for molecular analysis were taken in three replicates exclusively from the innermost part of the cores using sterile 5-ml syringes with cutoff tips. Due to differences in the lengths of the cores, only the upper 360-cm portions were directly compared. All subsamples were stored at −20°C until processing. Pore water was separated from sediment samples by centrifugation (5 min, 15,000 × *g*) using centrifuge tubes with inserted Teflon sieves. The resulting volume of pore water (approximately 10% [wt/wt] of sediment) was filtered through 0.2-μm membrane filters.

Geochemical parameters. Cores A to C were analyzed in terms of sedimentological sequence, total organic carbon content (TOC), dissolved organic carbon (DOC), ammonium, sulfate, and chloride concentrations. Core D was recovered to retrieve a corresponding methane profile after the main geochemical and microbiological analyses were already performed on cores A to C. Therefore, this core was analyzed only for sulfate, chloride, and methane concentrations.

The lithological description of cores A to C was done by visual inspection (Fig. 1). TOC was determined as the difference between total carbon analyzed by combustion in a CS-444 instrument (Leco Instruments GmbH, Mönchengladbach, Germany) and inorganic carbon measured with a CO_2 coulometer (UIC Inc., Joliet, IL). DOC was analyzed on a Multi N/C3000 instrument (Jena AG, Jena, Germany). A 400-μl aliquot of pore water was diluted with water, acidified with 2 N HCl, and purged with synthetic air to remove inorganic carbon. The samples were combusted at 850°C in synthetic air with CeO_2 as the catalyst. CO_2 was detected by a nondispersive infrared detector. For external calibration a dilution series of a DOC standard (CertiPUR; Merck, Darmstadt, Germany) was treated and analyzed in the same way as the pore water samples. Pore water sulfate and chloride concentrations were measured by ion chromatography with conductivity detection as described previously (41). Ammonium was determined photometrically (13). For measuring methane concentrations, 2 cm^3 of sediment was added immediately after sampling to 20 ml sodium hydroxide solution (2.5%) in gastight tubes. From the headspace, 20 μl gas was injected into a CX 3400 gas chromatograph (Varian Deutschland GmbH, Darmstadt, Germany) equipped with a capillary column (plot-fused silica column no. 7517, 25 m by 0.53 mm, Al_2O_3/KCl coated; Chromopack, Middleburg, The Netherlands) and measured by a flame ionization detector.

DNA extraction and PCR amplification. Genomic DNA was extracted from 0.5 g of sediment subsamples using the FastDNA SpinKit (Q-BIOgene, Carlsbad, CA). A 550-bp fragment of the bacterial 16S rRNA gene was amplified by using the primers 341f (5′-CCTACGGGAGGCAGCAG-3′) and 907r (5′-CCGTCAATTCCTTTGAGTTT-3′). The PCR protocol was described previously (7). A nested PCR was used for investigations on the archaeal community composition as described by Vetriani et al. (51). The primers for the amplification of the almost-complete archaeal 16S rRNA gene were S-D-Arch-0025-a-S-17 (5′-CTGGTTGATCCTGCCAG-3′) and S-*-Univ-1517-a-A-21 (5′-ACGGCTACCTTGTTACGACTT-3′). In contrast to the original procedure, the annealing time was set to 45 seconds and the elongation time to 1 minute. The nested PCR of a 550-bp fragment by primers S-D-Arch-0344-a-S-20 (5′-ACGGGGCGCAGCAGGCGCGA-3′) and 907r was performed with 35 cycles. PCR conditions for the amplification of a 500-bp 18S rRNA gene fragment by primers Euk1Af (5′-CTGGTTGATCCTGCCAG-3′) and Euk516r (5′-ACCAGACTTGCCCTCC-3′) were those described by Diez et al. (9). The elongation time was set to 1 minute. All PCRs were performed and checked by electrophoresis as described previously (56).

Denaturing gradient gel electrophoresis (DGGE) analysis. The PCR amplicons were purified and adjusted to a final volume of 10 μl by the MinElute PCR purification kit according to the manufacturer's instructions (QIAGEN, Hilden, Germany). Finally, loading buffer (40% [wt/vol] glycerol, 60% [wt/vol] 1× Tris-acetate-EDTA [TAE], and bromphenol blue) and samples were mixed in a ratio of 1:2.

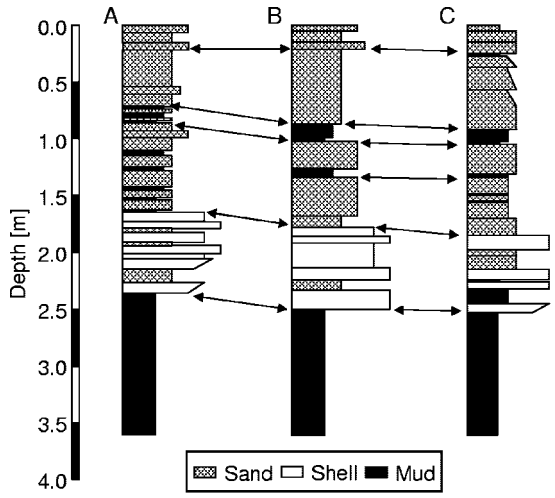

FIG. 1. Simplified lithological profiles of the three sediment cores. The widths of the bars indicate grain sizes. The arrows show characteristic layers that were used for correlating the cores. Sediment cores were collected in June 2002 (core A), October 2003 (core B), and February 2004 (core C).

DGGE was performed on an INGENYphorU-2 system (Ingeny, Goes, The Netherlands). PCR products of the bacterial 16S rRNA gene were loaded onto polyacrylamide gels (6%, wt/vol) in 1× TAE, with a denaturing gradient from 50 to 70% (with 100% denaturant corresponding to 7 M urea and 40% formamide). For the DGGE analysis of archaeal 16S rRNA gene fragments and 18S rRNA gene amplicons, the denaturing gradient was adjusted to 40 to 70%. Electrophoresis was performed at a constant voltage of 100 V and a temperature of 60°C for 20 h. After electrophoresis, the gels were stained for 2 h in 1× SybrGold solution (Molecular Probes, Eugene, Oreg.) in 1× TAE, washed for 20 min with distilled water, and documented using a digital imaging system (BioDocAnalyze; Biometra, Göttingen, Germany). The images are represented as Fig. S1 to S3 in the supplemental material.

The resulting band patterns were analyzed by cluster analysis using the software package GelComparII, version 2.5 (Applied Maths, St-Martens-Latem, Belgium). Since all lanes of a DGGE gel contain a characteristic degree of smear, a background subtraction was performed to make different lanes comparable. Therefore, a background scale of 5 to 20% was applied in the software package depending on the signal-to-noise ratio of the gel. The densitometric curves were compared using the Pearson coefficient (36). A position tolerance optimization was performed to fit the curves to the best possible match. We used the curve-based approach instead of comparing single bands as this type of analysis was shown to be more robust (11, 43). The unweighted-pair group method with arithmetic averages (46) was used to generate the dendrograms.

Sequence analysis. DGGE bands were excised for sequencing and treated as described previously (7). Single-strand sequencing was performed on a DNA Sequencing System 4000 (LI-COR Inc., Lincoln, Neb.) using IRDye800-labeled primers and the DYEnamic direct cycle sequencing kit (Amersham Biosciences, Little Chalfont, United Kingdom) in accordance with the manufacturer's instructions. Bands obtained by applying bacterial and archaeal primers were sequenced with primer 907r. For eukaryotic bands primer Euk516r was used. To affiliate the sequences to the closest phylotype or the most closely related and validly described species, they were compared to those in GenBank using the BLAST function of the National Center for Biotechnology Information server (www.ncbi.nlm.nih.gov).

The ARB program package (26) was used for the detailed phylogenetic analysis of the detected TF1 cluster (see Fig. S4 in the supplemental material). All archaeal sequences from the ARB database (release 2004) longer than 1,400 bp were used as the backbone for the phylogenetic tree constructed by the maximum-likelihood method. Shorter sequences (length: approximately 400 bp) obtained by sequencing of DGGE bands were added later to the final tree using the maximum-parsimony option of the ARB program. Alignment positions at which

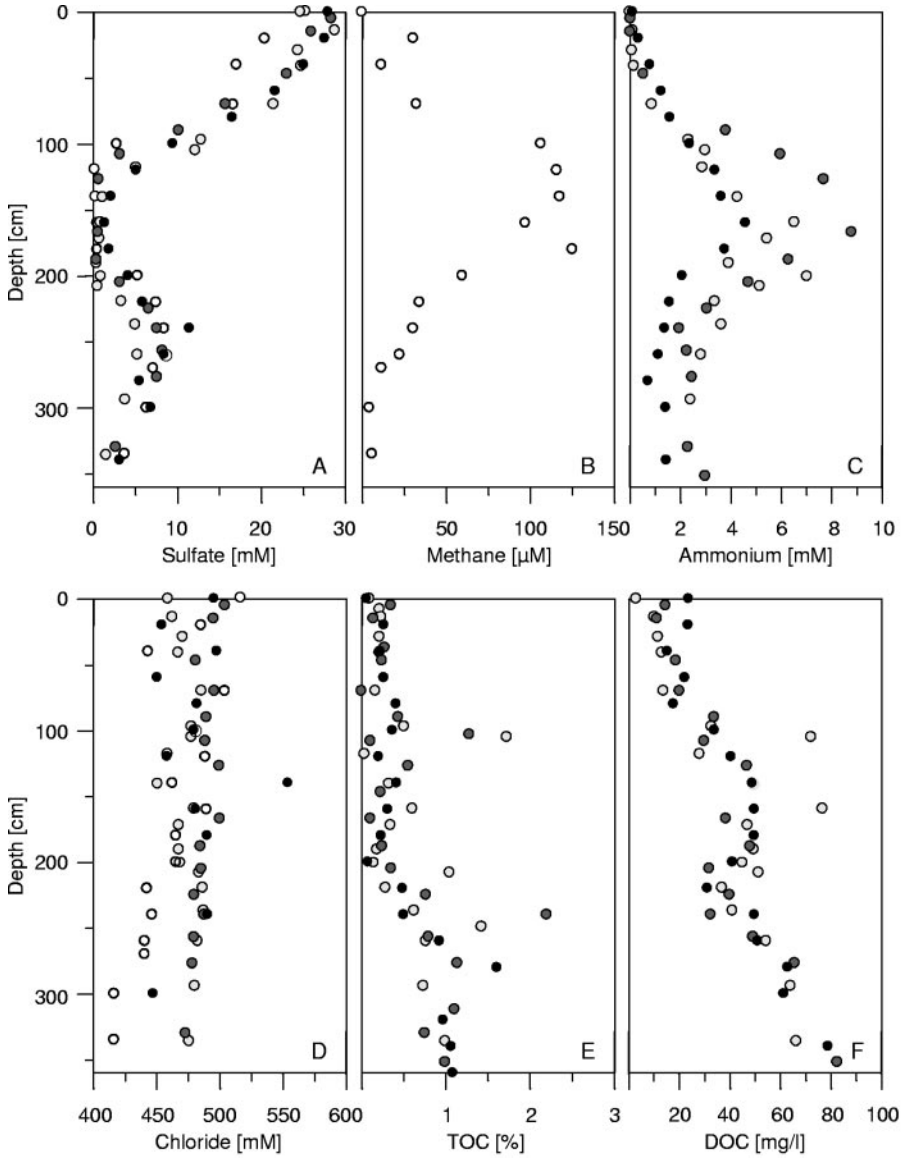

FIG. 2. Geochemical profiles along the sediment cores. A) Sulfate; B) methane; C) ammonium; D) chloride; E) TOC; F) DOC. Core A, black circles; core B, dark gray circles; core C, light gray circles; core D, open circles. The zone between 100 and 200 cm shows low sulfate values, high methane and ammonium values, and a higher ratio of DOC to TOC.

less than 50% of sequences of the entire data set had the same residues were excluded from the calculations to prevent mistakes in tree topology (26).

Nucleotide sequence accession numbers. All partial 16S rRNA gene sequences obtained in this study were deposited in the EMBL database under accession numbers AM072577 to AM072620. The 18S rRNA gene sequences were deposited under accession numbers AM072559 to AM072576.

RESULTS

Lithological characterization of the sampling site. The sampling site is located on a mixed tidal flat at the German North Sea coast. It was chosen due to its characteristic lithological profile, which comprises three different sedimentary units. Distinctive layers detected by sedimentological analysis allowed alignment of the individual cores taken during different sampling campaigns (Fig. 1). In the lowermost part, the cores comprised gray mud-rich sediments deposited mainly in a salt marsh environment (4). They were overlain by an interval rich in shell beds (ca. 180 to 250 cm in depth). The sediments in the upper part were sand dominated with thin intercalations of black mud and were deposited in a sand to mixed-tidal-flat environment. Minor differences in lithological composition indicate the patchiness of the habitat and were probably caused by small deviations of the sampling positions within the accuracy of the global positioning system (approximately 5 m). An age of approximately 600 years was estimated for the shell layers (D. Ziehe, personal communication), resulting in an average sedimentation rate of 22 to 30 cm per 100 years as reported by Kunz (24).

Geochemical profiles. The geochemical profiles of the cores were similar (Fig. 2). At the sediment surface, sulfate concen-

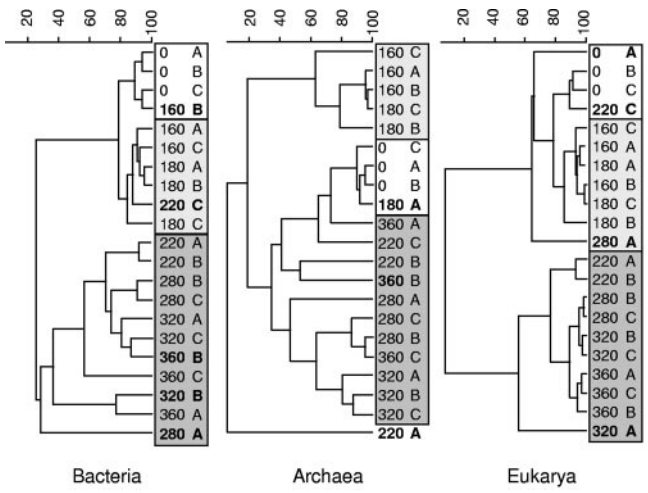

FIG. 3. Cluster analysis of DGGE band patterns from cores A to C obtained by the separation of specific PCR amplicons from *Bacteria*, *Archaea*, and *Eukarya*. The dendrograms were calculated by Pearson correlation and the unweighted-pair group method with arithmetic averages. The geochemically defined sediment horizons are indicated by different colors: white for the surface layer, light gray for the sulfate-free and methane-rich layers, and dark gray for the deeper layers including the deep sulfate maximum. Samples that affiliated to a different cluster are marked in boldface.

trations of about 30 mM were measured (Fig. 2A). Beneath 50 cm in depth, sulfate decreased rapidly to concentrations below 1 mM. At approximately 250 cm, a second maximum of pore water sulfate was detected, with concentrations ranging from 5.3 (core C) to 11.5 mM (core A). Sulfate was depleted beneath 400 cm, with concentrations below 0.2 mM (data not shown). The sulfate profile in core D showed the same shape as in the other cores. Therefore, the corresponding methane profile (Fig. 2B) determined exclusively for core D can be assumed to be representative for all cores.

Methane was detected along the anoxic part of the sediment column, showing concentrations below the detection limit in the surface sample only. The highest methane value (125 μM) was measured in the sulfate minimum zone (100 and 200 cm). In the deepest layer of core D (450 cm in depth), still 100 μM methane was detected (data not shown).

Maximum ammonium concentrations (4.6 to 8.8 mM) were found within the lower part of the sand-dominated interval and the upper shell layers (120 to 200 cm; Fig. 2C). Beneath this peak, concentrations did not decrease below 1 mM.

Almost constant chloride concentrations indicate that the pore water in the three different lithological compartments of the cores is not strongly influenced by an inflow of groundwater from the nearby mainland (Fig. 2D).

The TOC in the sand-dominated sediments was generally below 0.5% (Fig. 2E). Higher values (up to 1.3%) were found only for thin intercalations of black mud. In the gray mud interval below the shell layers, the TOC content varied between 0.8 and 1.9%. DOC values increased with depth except in the layers between 100 and 200 cm (Fig. 2F). Here, a slight accumulation of up to 70 mg DOC per liter pore water was measured.

Molecular investigation with domain-specific primers. Clustering of DGGE banding patterns revealed two main clusters for *Bacteria*, *Archaea*, and *Eukarya* (Fig. 3). These clusters were defined by less than 20% pattern similarity. Specific primers targeting bacterial and eukaryotic diversity yielded one main cluster for the upper 180 cm and a second one for the layers from 220 cm downwards. PCR using *Archaea*-specific primers resulted in a separate cluster for the sulfate-depleted layers at 160 and 180 cm in depth.

These major clusters were structured, and subclusters could be identified. In particular, patterns derived from bacterial and eukaryotic communities from the surface and from the deeper sand-dominated layers (160 to 180 cm) were clearly distinguishable. These clusters appeared to be very stable and almost showed no changes during the three sampling campaigns. In contrast, DGGE band patterns of communities within the deeper layers appeared to be more diverse. Here, no conspicuous subclusters could be identified.

Spatial variations in community composition were reflected by the affiliation of distinct sediment layers to different ones of other cores (e.g., core B; depth, 160 cm). One sample (core C; depth, 220 cm) seemed to be an outlier and neither showed similarities to corresponding layers nor was affiliated to other clusters.

Phylogenetic affiliation of dominant bacterial phylotypes. The dominant representatives of the three domains were identified by sequence analysis of excised DGGE bands. Twenty-six bacterial bands have been unambiguously sequenced (Table 1). These were affiliated to *Proteobacteria*, *Actinobacteria*, *Bacteroidetes*, *Firmicutes*, *Spirochaetes*, and *Chloroflexi*. Interestingly, the total number of phylotypes that have been detected by the methods applied did not decrease with depth. The depth distribution and compositional changes of these groups reflect the clusters obtained from the DGGE band patterns. For example, *Gammaproteobacteria* were found almost exclusively in the upper sand-dominated interval, whereas *Firmicutes*, *Bacteroidetes*, and *Chloroflexi* were detected mainly within the deepest layers at 220 cm and below. Although the sequences have been affiliated easily with main bacterial phyla, only two of them showed similarities of more than 95% to cultured organisms: the gammaproteobacterium *Thioalkalispira microaerophila*^{T} and the deltaproteobacterium *Pelobacter carbinolicus*. The majority of the sequences were only remotely related to those of cultured organisms (less than 90% similarity).

Affiliation of dominant archaeal phylotypes. Fourteen bands were excised and sequenced after DGGE analysis of amplicons obtained by the application of *Archaea*-specific primers (Table 2). All of them yielded reliable sequences that were mostly affiliated with methanogenic archaea. Three of these sequences were closely related (more than 95% similarity) to *Methanogenium cariaci*^{T} and *Methanolobus oregonensis*, while nine sequences revealed less than 90% of sequence similarity to cultured archaea but were nevertheless phylogenetically related to previously cultivated methanogens. As for the *Bacteria*, the phylogenetic affiliation of the detected archaeal sequences changed with depth. Sequences belonging to the *Methanosarcinales* prevailed along the entire sediment column, whereas those of *Methanomicrobiales* were detected within the upper 180 cm. Sequences affiliated to *Methanobacteriales* and *Thermococcales* were found in deeper layers.

TABLE 1. Overview of eubacterial phylotypes detected by PCR-DGGE[a]

Phylogenetic affiliation	Closest described relative		Closest phylotype		Band no. at depth (cm) of:		
	Species or strain (accession no.)	Sim[b] (%)	Organism, clone, or band	Sim (%)	0	160–180	220–360
α-*Proteobacteria*	*Blastochloris sulfoviridis* RN1	83	Unc.[c] bacterium clone CS8.15	96			14
γ-*Proteobacteria*	*Alkalispirillum mobile* (AF114783)	90	Unc. bacterium isolate JH10 C59	95	+[d]	07	
	Alkalispirillum mobile (AF114783)	92	Unc. γ-proteobacterium band GWS-SE-4	96	08/11	+	
	Alkalispirillum mobile (AF114783)	91	Unc. γ-proteobacterium band GWS-SE-5	97	+	12	
	Thioalkalispira microaerophila ALEN 1	95	Unc. γ-proteobacterium clone SIMO-2435	97	+	10	
δ-*Proteobacteria*	*Desulfobacca acetoxidans* (AF002671)	85	Unc. bacterium gene AB177169	98			27
	Desulfobulbus propionicus DSM 2032	84	Unc. bacterium isolate DGGE-BAC-3	94			04
	Desulfococcus multivorans DSM 2059	92	Unc. δ-proteobacterium 63-2	96			22
	Haliangium tepidum (AB062751)	90	Unc. δ-proteobacterium band GWS-a12-PA	99	+	20a-b	+
	Pelobacter carbinolicus DSM 2380	95	Unc. δ-proteobacterium DGGE gel band 8	96	19		
Actinobacteria	*Streptomyces laceyi* c765	86	Unc. actinobacterium gene clone Y193	98	+	24	
Bacteriodetes	*Flexibacter canadensis* (M62793)	91	Unc. bacterium gene clone OHKB2.48	97			03
	Tenacibaculum maritimum IFO 15946	94	*Flavobacteriaceae* bacterium T15	99		+	01
	Marinilabilia salmonicolor NCIMB 2216	90	Unc. *Bacteroidetes* clone SIMO-1682	93			02
Chloroflexi	*Anaerolinea thermophila* UNI-1^T	85	Unc. bacterium Seq2 (S1)	98			25
	Anaerolinea thermophila STL-6-O1	85	Unc. green nonsulfur bacterium P. palm C37	91			13
	"*Dehalococcoides ethenogenes*" 195	86	Unc. bacterium clone ER-E10-19	95		+	05/06
	"*Dehalococcoides ethenogenes*" 195	88	Unc. bacterium clone Napoli-3B-22	97		+	09
	"*Dehalococcoides ethenogenes*" 195	87	Unc. bacterium clone Urania-2B-30	97			17
	"*Dehalococcoides ethenogenes*" 195	87	Unc. bacterium gene clone OHKB2.17	99			21
	"*Dehalococcoides ethenogenes*" 195	87	Unc. *Chloroflexi* ODP1176A6H_1_B	96			16a-c
	"*Dehalococcoides ethenogenes*" 195	87	Unc. eubacterium t0.6.f	94			18
Firmicutes	*Caldicellulosiruptor owensensis* (U80596)	83	Unc. bacterium gene clone ITKB-228	96			26
	Cryptanaerobacter phenolicus LR7.2^T	86	Unc. bacterium gene clone OHKB2.40	95			23
	Garciella nitratireducens Met79^T	91	Unc. bacterium clone 42-B47	92			15
Spirochetes	*Spirochaeta africana* DSM 8902	87	Unc. spirochete clone SIMO-1951	98	+	+	28

[a] For each phylotype, the most closely related sequence, the closest cultivated organism, and the appearance of the bands with depth are given. Band numbers correspond to those of Fig. S1 in the supplemental material.
[b] Sim, similarity.
[c] Unc., uncultured.
[d] +, band present but not sequenced.

Some of the sequences amplified by PCR using *Eukarya*-specific primers were in fact affiliated to *Archaea* (Table 2). An increase in the number of prokaryotic 16S rRNA gene sequences with depth was already visible on the agarose gel that was used for testing the PCR efficiency. A 50-base-pair-shorter band, caused by size variations between the prokaryotic 16S rRNA and the eukaryotic 18S rRNA gene amplicons, was additionally detectable in samples from 160 cm downwards only (data not shown). These sequences formed an isolated group within the *Euryarchaeota* and were only remotely related to any database entry (less than 90% homology). The closest cultivated organisms by the BLAST score were distributed over the groups of *Archaeoglobales*, *Methanobacteriales*, *Methanococcales*, and *Thermococcales*. By phylogenetic analysis using the software ARB (26), it was found that these sequences form a new isolated cluster within the *Euryarchaeota*, assigned as "tidal-flat cluster 1" (TF1).

Affiliation of dominant eukaryotic phylotypes. Besides the five archaeal phylotypes detected by *Eukarya*-specific primers, 18 sequences of DGGE bands were affiliated to *Eukarya* (Table 3). These were mainly found in the upper part of the DGGE gel; archaeal TF1 sequences were found in the lower section. Most of the *Eukarya* were affiliated with those of grazing microorganisms such as *Ciliophora*, *Gastrotricha*, *Euglenozoa*, and *Platyhelminthes* or with deposit feeders such as *Arthropoda*, *Nematoda*, and the diatom-feeding *Phagomyxa* (*Plasmadiophorida*). Five sequences showed more than 95% homology to those of identified eukaryotic organisms. Three other sequences that were detected within the deeper sediments only (bands 55, 61, and 65) were affiliated to a novel kingdom of supposedly anaerobic eukarya, which was described for a Californian tidal flat by Dawson and Pace (6). Two other sequences showed a reasonable homology only over a very short part of the 18S rRNA gene. One of them revealed the highest similarity to *Diplonema ambulator* strain ATCC 50223 (76 of 332 bp) and the other one to *Spirostomum ambiguum* (51 of 336 base pairs). In these two cases, a sound phylogenetic analysis was not yet possible because of the low number of eukaryotic 18S rRNA gene entries in the databases. The number of detected phylotypes decreased with depth from 10 at the surface to 5 beneath 160 cm in depth. All phylotypes except *Gyratrix hermaphroditus* were detected in a single depth cluster only.

DISCUSSION

Our study has demonstrated that the composition of microbial communities is correlated to sediment horizons with distinctive lithological and geochemical properties. Bacterial communities appeared to be affected mainly by the availability and quality of carbon sources, while archaeal-community composition correlated with methane and sulfate concentrations.

TABLE 2. Overview of archaeal phylotypes detected by PCR-DGGE[a]

Phylogenetic affiliation	Closest described relative		Closest phylotype		Band no.[d] at depth (cm) of:		
	Species or strain (accession no.)	Sim[b] (%)	Organism or clone	Sim (%)	0	160–180	220–360
Archaeoglobales	*Ferroglobus placidus* (AF220166)	84	Unc.[c] euryarchaeote clone 1a_D3	86			66a-b*
Methanobacteriales	*Methanobrevibacter oralis* DSM 7256	84	Unc. archaeon clone Napoli-3A-03	98			35
	Methanothermobacter thermoflexus DSM 7268	86	Unc. archaeon clone Napoli-2A-15	88			64*
Methanococcales	*Methanococcus vulcanis* M7	87	Unc. archaeon clone G26_C50	87			62a-b*
Methanomicrobiales	*Methanogenium cariaci* DSM 1497	96	Unc. archaeon 2C130	98	42a	42b	
	Methanogenium cariaci DSM 1497	96	Unc. *Methanogenium* sp. clone LH23	98	44		
	Methanogenium frigidum OCM 469	92	Unc. archaeon ACE4_A	95		45a+b	
Methanosarcinales	*Methanococcoides burtonii* DSM 6242^T	83	Unc. archaeon AT425_ArB9	94			37
	Methanococcoides burtonii DSM 6242^T	94	Unc. archaeon clone V.8.ArB2	94	34/39	+	
	Methanohalophilus portucalensis FDF1	86	Unc. archaeon 19b-9	86			40
	Methanolobus oregonensis WAL1	95	Unc. archaeon ZAR122	98	36/38	+	
	Methanosarcina lacustris MS	85	Unc. archaeon clone BS-S-D7	96			31/33a-c
	Methanosarcina lacustris MS	85	Unc. archaeon clone BS-S-D7	95			43a-b
	Methanosarcina lacustris MS	84	Unc. archaeon clone V.8.ArC17	94			41
	Methanothrix thermophila CALS-1	84	Unc. archaeon clone DR91PCA16SCT1	97			29
Thermococcales	*Pyrococcus furiosus* DSM 3638	85	Unc. archaeon gene IAN1-71	84		68*	69*
	Pyrococcus furiosus DSM 3638	83	Unc. archaeon TA02	84		67*	+
	Pyrococcus horikoshii OT3	87	Unc. archaeon AT425_ArB9	94			30
	Thermococcus gammatolerans EJ3	83	Unc. archaeon AT425_ArB9	93			32

[a] All phylotypes correspond to the phylogenetic group of *Euryarchaeota.* For each phylotype, the most closely related sequence, the closest cultivated organism, and the appearance of the bands with depth in the three cores are given. Band numbers correspond to those of Fig. S2 and S3 in the supplemental material.
[b] Sim, similarity.
[c] Unc., uncultured.
[d] +, band present but not sequenced. *, archeal sequence (TF1) found with primers for *Eukarya.*

These patterns were most likely stable over several years. Minor differences may be caused by the patchiness of the tidal-flat system, small variations in depth determination, or pitfalls intrinsic to the molecular approach, for example, preferential amplification or variable primer specificities (53). However, at least two samples from corresponding layers in different cores, hence from different sampling campaigns, showed a congruent community composition. The general consistence between the deeper layers of the investigated sediment cores in terms of geochemical and microbial community profiles indicates the stability of the tidal-flat system.

Methanogenic community composition reflects pore water sulfate and methane concentrations. The occurrence of methanogens throughout the whole sediment column is reflected by the methane profile, as methane was detected in every anoxic-sediment sample. The distribution of *Archaea* can be interpreted as a result of competition with sulfate-reducing bacteria. Archaeal sequences found at the surface and within the sulfate-free layers (160 and 180 cm in depth) are affiliated to those of the generally hydrogenotrophic *Methanomicrobiales*. These organisms are known to compete directly with sulfate reducers for hydrogen (33). The coexistence (32) found in the anoxic surface layer (beneath 5 mm in depth [2]) is probably due to a substrate surplus that may be generated by exudates of benthic photosynthetic organisms.

The occurrence of *Methanomicrobiales* in the sulfate-free layers can be explained by less competition with sulfate reducers. Members of the *Methanosarcinales*, detected along the whole sediment column, are able to avoid competition by utilizing substrates like methylamines (27) or dimethylsulfide (50) that are generally neglected by most other physiological groups. These compounds are typically released during the decay of algae or other organisms and are mostly available near the sediment surface. In deeper layers, however, complex methylated aromatic compounds like humic acids or peat components (19) are a potential source of energy. *Methanosarcina* strains were shown to demethylate aromatic compounds like toluene sulfonate (44) or to demethoxylate lignin monomers (37).

Organic carbon governs bacterial communities. The electron donor appears to be more relevant for bacterial communities in subsurface sediments than the electron acceptor. Poor quality of organic-matter supply is a common feature of subsurface habitats down to hundreds of meters below the seafloor (3, 5, 16, 35, 54). Here, the reduced availability of organic carbon and its low biodegradability have the most pronounced influence on the community composition. From age determinations it can be inferred that the organic material in the subsurface of the tidal flat must be highly recalcitrant due to degradation and alteration during both sedimentation and burial (52). The correlation of the TOC content to the occurrence of mud further indicates that sorption by fine particles plays an important role in the preservation of organic matter (52) and reduces the bioavailability. The estimation of the DOC/TOC ratio gave almost equal results for the surface and deeper mud layers, whereas higher ratios were estimated for depths between 100 and 200 cm. This DOC peak corresponds well to the elevated ammonium values within this zone. Ammonium is likely to accumulate due to degradation of recalcitrant organic matter in the absence of potential electron acceptors for oxidation. A very similar correlation was found by Komada et al. in anoxic coastal sediments (22) and is a good indication of metabolically active microbial communities.

The detected bacterial communities appear to be dominated by fermenters and syntrophic bacteria, which are known to represent the majority of microorganisms in anoxic sediments (42). Even though total cell counts decreased slightly from 1×10^9 cells per g sediment at the surface to 4×10^7 cells per g sediment at 450 cm (23), they seemed to be equally distributed as no decreasing band numbers were found by DGGE analysis (see Fig. S1 in the supplemental material). Since fermenting

TABLE 3. Overview of eukaryotic phylotypes detected by PCR-DGGE[a]

Phylogenetic affiliation	Closest described relative		Closest phylotype		Band no. at depth (cm) of:		
	Species or strain (accession no.)	Sim[b] (%)	Organism, clone, or band	Sim (%)	0	160–180	220–360
Alveolata							
Apicomplexa	*Cryptosporidium struthionis* (AJ697751)	92	Unc.[c] marine eukaryote isolate JPeuk-65	93		+[d]	49a-b
Ciliophora	*Orthodonella apohamatus* (DQ232761)	95	*Orthodonella apohamatus* (DQ232761)	95	50		
	Spirostomum ambiguum (L31518)	94	Unc. *Amoebophrya* clone F	94	46		
Dinophyceae	*Prorocentrum micans* (AY833514)	92	Unc. marine eukaryote clone M3_18E07	97		54	+
	Thecadinium dragescoi (AY238479)	92	*Thecadinium dragescoi* (AY238479)	92		51	
Cryothecomonas	*Cryothecomonas longipes* (AF290540)	89	Unc. eukaryote isolate BS_DGGE-Euk-4	90			47
Euglenozoa	*Diplonema ambulator* strain ATCC 50223	98	Unc. eukaryote clone BAQA65	93			65
	Euglena agilis (AF115279)	88	*Euglena agilis* (AF115279)	88	63		
Fungi	*Monoblepharella* sp. strain M15	93	Unc. eukaryote clone BOLA187	93		55	
Metazoa							
Arthropoda	*Cytheromorpha acupunctata* (AB076630)	94	*Cytheromorpha acupunctata* (AB076630)	94	56		
	Leptocythere lacertosa (AB076631)	95	*Leptocythere lacertosa* (AB076631)	95	60		
Cnidaria	*Junceella aquamata* (AY962535)	94	*Junceella aquamata* (AY962535)	94	48		
Gastrotricha	*Neodasys ciritus* (AY228127)	95	*Neodasys ciritus* (AY228127)	95	59		
Nematoda	*Dichromadora* sp. strain BHMM-2005	96	*Dichromadora* sp. strain BHMM-2005	96	58		
Platyhellminthes	*Gyratrix hermaphroditus* (AJ012510)	92	*Gyratrix hermaphroditus* (AJ012510)	92	52a	52b	
Tardigrada	*Pseudechiniscus islandicus* (AY582119)	92	*Pseudechiniscus islandicus* (AY582119)	92	57		
Nucleariidae	*Nuclearia moebiusi* CCAP 1552/3	89	Unc. eukaryote clone BOLA187	90		61	
Plasmodiophorida	*Phagomyxa bellerocheae* (AF310903)	89	*Phagomyxa bellerocheae* (AF310903)	89			53

[a] For each phylotype, the most closely related sequence, the closest cultivated organism, and the appearance of the bands with depth are given. Band numbers correspond to those in Fig. S3 in the supplemental material.
[b] Sim, similarity.
[c] Unc., uncultured.
[d] +, band present but not sequenced.

microorganisms are independent of sulfate, they are uniformly distributed in the upper 200 cm of the sediment, including the sulfate minimum zone. On the other hand, by releasing fermentation products they provide substrates for terminal oxidizers like sulfate reducers and methanogens (12). Sulfate-reducing bacteria, in turn, rely on the availability of sulfate but do not obviously belong to the most abundant bacterial groups in sediments, even in those exhibiting intense sulfate reduction (25). Changes in the sulfate-reducing community are likely to occur but probably remain undetected by the chosen domain-specific 16S rRNA gene approach. To link phylogenetic compositions within the different horizons with physiological information, the analysis of functional genes is an aim for future studies.

Indications for anaerobic methane oxidation. The bell-shaped curve of the sulfate peak points to a thin layer of lateral pore water inflow from nearby tidal creeks as the source of sulfate. The detected methane profile is opposed to the sulfate profile. Therefore, the geochemical profile of site Neuharlingersieler Nacken is characterized by sulfate-methane transition zones at 100 and 200 cm in depth. The sulfate and methane profiles provide circumstantial evidence for anaerobic methane oxidation. This process is thought to be catalyzed by consortia of methanogenic archaea and sulfate-reducing bacteria as first described for deep-sea sites (1). However, the consortia were also found in a recent investigation of a nearby tidal flat at a 12-cm sediment depth (18). In the present study, sequences affiliated to members of the archaeal ANME group and to *Desulfosarcinales* or *Desulfococcales*, which form these consortia, were not detected. However, both sulfate reducers and methanogens are present in the sulfate-methane transition zones. Therefore, their involvement in the oxidation of methane within the tidal-flat sediment has to be considered.

The detection of a novel archaeal cluster ("tidal-flat cluster 1"). In deeper sediment layers a new phylogenetic cluster of archaea, labeled TF1, was detected by DGGE analysis of 400-bp 16S rRNA gene fragments (see Fig. S4 in the supplemental material). These sequences were obtained by using primers that should specifically amplify the first 500 bp for eukaryotic 18S rRNA genes (9, 45). We are aware that comparing full 16S rRNA gene sequences would give more-comprehensive phylogenetic information. On the other hand, Stackebrandt and Rainey have demonstrated that partial 16S rRNA gene sequences of about 500 nucleotides can be sufficient for a phylogenetic assignment down to the genus level (47). For the TF1 cluster, in fact, it is difficult to obtain a full 16S rRNA gene sequence since the *Archaea*-specific reverse primer (S-*-Univ-1517-a-A-21) needed for amplification of the almost-complete gene seemingly does not match. This might be one reason why this cluster was not detected by our *Archaea*-specific approach or by studies based on the analysis of clone libraries. About the physiological properties of their members only speculation is possible, since similarities to other archaeal sequences are less than 87%. This example, however, demonstrates that new phylotypes can be detected in a given habitat if unusual primer combinations are used.

Depth distribution of *Eukarya*. In our investigations, the "*Eukarya*-specific" primer pair was applied for the first time to subsurface habitats. Surprisingly, grazing eukarya were detectable in deeper layers, even though their diversity decreased with depth. It is feasible that at least part of the eukaryotic community detected is due to the presence of resting stages, like cysts, that can remain viable for long periods. But even if active eukaryotic communities were present in the deep layers, their number must be small since the bacterial production that is needed to support heterotrophic protists is supposedly

rather low. On the other hand, the archaeal TF1 cluster in deeper layers might hinder the detection of eukaryotic communities by DGGE analysis. Cluster analysis by the eukaryotic DGGE approach reflects the distribution of both eukarya and the TF1 cluster. Recent studies demonstrated a high diversity of viable anaerobic eukaryotes within surface sediments (6, 14, 48). However, whether eukaryotic microorganisms are active in anoxic environments remains elusive as long as observations of in situ activities are missing. So far, the domain of *Eukarya* is not sufficiently investigated in the subsurface and needs more attention in future studies.

ACKNOWLEDGMENTS

We thank the crew of the RV Senckenberg and Maik Wilsenack for technical support during coring. We thank Alexander Bartholomä for geological advice and Katja Ziegelmüller for her help in sequencing DGGE bands. Elke Freese and Willm Martens-Habena are greatfully acknowledged for measuring organic carbon and analyzing pore water ammonium. For instructions for measuring methane and pore water sulfate we thank Yvonne Hilker and Melanie Beck.

This work is part of the research group on "BioGeoChemistry of Tidal Flats," supported by the Deutsche Forschungsgemeinschaft.

REFERENCES

1. **Boetius, A., K. Ravenschlag, C. J. Schubert, D. Rickert, F. Widdel, A. Gieseke, R. Amann, B. B. Jørgensen, U. Witte, and O. Pfannkuche.** 2000. A marine microbial consortium apparently mediating anaerobic oxidation of methane. Nature **407:**623–626.
2. **Böttcher, M. E., B. Hespenheide, E. Llobet-Brossa, C. Beardsley, O. Larsen, A. Schramm, A. Wieland, G. Böttcher, U.-G. Berninger, and R. Amann.** 2000. The biogeochemistry, stable isotope geochemistry, and microbial community structure of a temperate intertidal mudflat: an integrated study. Continental Shelf Res. **20:**1749–1769.
3. **Chandler, D. P., F. J. Brockman, T. J. Bailey, and J. K. Fredrickson.** 1998. Phylogenetic diversity of archaea and bacteria in a deep subsurface paleosol. Microb. Ecol. **36:**37–50.
4. **Chang, T. S., A. Bartholomae, E. Tilch, and B. W. Flemming.** 2003. Recent development of the back-barrier tidal basin behind the island of Spiekeroog in the East Frisian Wadden Sea. Ber. Forschungszentrum Terramare **12:**43–44.
5. **Coolen, M. J. L., H. Cypionka, A. M. Sass, H. Sass, and J. Overmann.** 2002. Ongoing modification of Mediterranean Pleistocene sapropels mediated by prokaryotes. Science **296:**2407–2410.
6. **Dawson, S. C., and N. R. Pace.** 2002. Novel kingdom-level eukaryotic diversity in anoxic environments. Proc. Natl. Acad. Sci. USA **99:**8324–8329.
7. **Del Panno, M., I. S. Morelli, B. Engelen, and L. Berthe-Corti.** 2005. Effect of petrochemical sludge concentrations on microbial communities during a soil bioremediation process. FEMS Microbiol. Ecol. **53:**305–316.
8. **D'Hondt, S., B. B. Jørgensen, D. J. Miller, A. Batzke, R. Blake, B. A. Cragg, H. Cypionka, G. R. Dickens, T. Ferdelman, K.-U. Hinrichs, N. G. Holm, R. Mitterer, A. Spivack, G. Wang, B. Bekins, B. Engelen, K. Ford, G. Gettemy, S. D. Rutherford, H. Sass, C. G. Skilbeck, I. W. Aiello, G. Guerin, C. H. House, F. Inagaki, P. Meister, T. Naehr, S. Niitsuma, R. J. Parkes, A. Schippers, D. C. Smith, A. Teske, J. Wiegel, C. N. Padilla, and J. L. S. Acosta.** 2004. Distributions of microbial activities in deep subseafloor sediments. Science **306:**2216–2221.
9. **Diez, B., C. Pedros-Alio, T. L. Marsh, and R. Massana.** 2001. Application of denaturing gradient gel electrophoresis (DGGE) to study the diversity of marine picoeukaryotic assemblages and comparison of DGGE with other molecular techniques. Appl. Environ. Microbiol. **67:**2942–2951.
10. **Dittman, S.** 1999. The Wadden Sea ecosystem: stability, properties and mechanism. Springer, New York, N.Y.
11. **Ferrari, V. C., and J. T. Hollibaugh.** 1999. Distribution of microbial assemblages in the central Arctic Ocean basin studied by PCR/DGGE: analysis of a large data set. Hydrobiologia **401:**55–68.
12. **Garcia, J.-L., B. K. C. Patel, and B. Ollivier.** 2000. Taxonomic, phylogenetic, and ecological diversity of methanogenic *Archaea*. Anaerobe **6:**205–226.
13. **Grasshoff, K., K. Kremling, and M. Erhard.** 1999. Methods of seawater analysis, 3rd ed. Wiley-VCH. New York, N.Y.
14. **Hamels, I., K. Sabbe, K. Muylaert, C. Barranguet, C. Lucas, P. Herman, and W. Vyverman.** 1998. Organisation of microbenthic communities in intertidal estuarine flats, a case study from the Molenplaat (Westerschelde Estuary, The Netherlands). Eur. J. Protistol. **34:**308–320.
15. **Inagaki, F., Y. Sakihama, A. Inoue, C. Kato, and K. Horikoshi.** 2002. Molecular phylogenetic analyses of reverse-transcribed bacterial rRNA obtained from deep-sea cold seep sediments. Environ. Microbiol. **4:**277–286.
16. **Inagaki, F., M. Suzuki, K. Takai, H. Oida, T. Sakamoto, K. Aoki, K. H. Nealson, and K. Horikoshi.** 2003. Microbial communities associated with geological horizons in coastal subseafloor sediments from the Sea of Okhotsk. Appl. Environ. Microbiol. **69:**7224–7235.
17. **Inagaki, F., K. Takai, H. Hirayama, Y. Yamato, K. H. Nealson, and K. Horikoshi.** 2003. Distribution and phylogenetic diversity of the subsurface microbial community in a Japanese epithermal gold mine. Extremophiles **7:**307–317.
18. **Ishii, K., M. Mußmann, B. J. MacGregor, and R. Amann.** 2004. An improved fluorescence *in situ* hybridization protocol for the identification of bacteria and archaea in marine sediments. FEMS Microbiol. Ecol. **50:**203–212.
19. **Killops, S. D., and V. J. Killops.** 2005. Introduction to organic geochemistry, 2nd ed. Blackwell Publishing, Malden, Mass.
20. **Kim, B.-S., H.-M. Oh, H. Kang, and J. Chun.** 2005. Archaeal diversity in tidal flat sediment as revealed by 16S rDNA analyis. J. Microbiol. **43:**144–151.
21. **Kim, B.-S., H.-M. Oh, H. Kang, S.-S. Park, and J. Chun.** 2004. Remarkable bacterial diversity in the tidal flat sediment as revealed by 16S rDNA analysis. J. Microbiol. Biotechnol. **14:**205–211.
22. **Komada, T., C. E. Reimers, G. W. Luther III, and D. J. Burdige.** 2004. Factors affecting dissolved organic matter dynamics in mixed-redox to anoxic coastal sediments. Geochim. Cosmochim. Acta **68:**4099–4111.
23. **Köpke, B., R. Wilms, B. Engelen, H. Cypionka, and H. Sass.** 2005. Microbial diversity in coastal subsurface sediments: a cultivation approach using various electron acceptors and substrate gradients. Appl. Environ. Microbiol. **71:**7819–7830.
24. **Kunz, H.** 1993. Klimaänderungen und ihre Folgen für Wasserhaushalt, Gewässernutzung und Gewässerschutz, 97–136. *In* H. J. Schellnhuber and H. Sterr (ed.), Klimaänderung und Küste. Springer, Berlin, Germany.
25. **Llobet-Brossa, E., R. Rabus, M. E. Böttcher, M. Könneke, N. Finke, A. Schramm, R. L. Meyer, S. Grötzschel, R. Rossello-Mora, and R. Amann.** 2002. Community structure and activity of sulfate-reducing bacteria in an intertidal surface sediment: a multi-method approach. Aquat. Microb. Ecol. **29:**211–226.
26. **Ludwig, W., O. Strunk, R. Westram, L. Richter, H. Meier, Yadhukumar, A. Buchner, T. Lai, S. Steppi, G. Jobb, W. Forster, I. Brettske, S. Gerber, A. W. Ginhart, O. Gross, S. Grumann, S. Hermann, R. Jost, A. Konig, T. Liss, R. Lussmann, M. May, B. Nonhoff, B. Reichel, R. Strehlow, A. Stamatakis, N. Stuckmann, A. Vilbig, M. Lenke, T. Ludwig, A. Bode, and K.-H. Schleifer.** 2004. ARB: a software environment for sequence data. Nucleic Acids Res. **32:**1363–1371.
27. **Madigan, M. T., J. M. Martinko, and J. Parker.** 2003. Biology of microorganisms, 10th ed. Pearson Education, Inc. Upper Saddle River, N.J.
28. **Moreira, D., and P. Lopez-Garcia.** 2002. The molecular ecology of microbial eukaryotes unveils a hidden world. Trends Microbiol. **10:**31–38.
29. **Musslewhite, C. L., M. J. McInerney, H. Dong, T. C. Constott, M. Green-Bloom, D. Swift, and S. MacNaughton.** 2003. The factors controlling microbial distribution and activity in the shallow subsurface. Geomicrobiol. J. **20:**245–261.
30. **Mußmann, M., K. Ishii, R. Rabus, and R. Amann.** 2005. Diversity and vertical distribution of cultured and uncultured deltaproteobacteria in an intertidal mud flat of the Wadden Sea. Environ. Microbiol. **7:**405–418.
31. **Newberry, C. J., G. Webster, B. A. Cragg, R. J. Parkes, A. J. Weightman, and J. C. Fry.** 2004. Diversity of prokaryotes and methanogenesis in deep subsurface sediments from the Nankai Trough, ocean drilling program leg 190. Environ. Microbiol. **6:**274–287.
32. **Oremland, R. S., and S. Polcin.** 1982. Methanogenesis and sulfate reduction: competitive and noncompetitive substrates in estuarine sediments. Appl. Environ. Microbiol. **44:**1270–1276.
33. **Oremland, R. S., and B. F. Taylor.** 1977. Sulfate reduction and methanogenesis in marine sediments. Geochim. Cosmochim. Acta **42:**209–214.
34. **Parkes, R. J., B. A. Cragg, S. J. Bale, J. M. Getliff, K. Goodman, P. A. Rochelle, J. C. Fry, A. J. Weightman, and S. M. Harvey.** 1994. Deep bacterial biosphere in Pacific Ocean sediments. Nature **371:**410–413.
35. **Parkes, R. J., G. Webster, B. A. Cragg, A. J. Weightman, C. J. Newberry, T. G. Ferdelman, J. Kallmeyer, B. B. Jørgensen, I. W. Aiello, and J. C. Fry.** 2005. Deep sub-seafloor prokaryotes stimulated at interfaces over geological time. Nature **436:**390–394.
36. **Pearson, K.** 1926. On the coefficient of racial likeliness. Biometrika **18:**105–117.
37. **Phelps, C. D., and L. Y. Young.** 1997. Microbial metabolism of the plant phenolic compounds ferulic and syringic acids under three anaerobic conditions. Microb. Ecol. **33:**206–215.
38. **Poremba, K., U. Tillmann, and K. J. Hesse.** 1999. Tidal impact on planktonic primary and bacterial production in the German Wadden Sea. Helgoland Mar. Res. **53:**19–27.
39. **Rasmussen, H., and B. B. Jørgensen.** 1992. Microelectrode of seasonal oxygen uptake in a coastal sediment: role of molecular diffusion. Mar. Ecol. Prog. Ser. **81:**289–303.
40. **Reise, K.** 2002. Sediment mediated species interactions in coastal waters. J. Sea Res. **48:**127–141.
41. **Sass, A. M., H. Sass, M. J. L. Coolen, H. Cypionka, and J. Overmann.** 2001.

Microbial communities in the chemocline of a hypersaline deep-sea basin (Urania Basin, Mediterranean Sea). Appl. Environ. Microbiol. **67:**5392–5402.
42. **Schink, B.** 2002. Synergistic interactions in the microbial world. Antonie Leeuwenhoek **81:**257–261.
43. **Selje, N., and M. Simon.** 2003. Composition and dynamics of particle-associated and free-living bacterial communities in the Weser Estuary, Germany. Aquat. Microb. Ecol. **30:**221–237.
44. **Shcherbakova, V. A., K. S. Laurinavichyu, A. M. Lysenko, N. E. Suzina, and V. K. Akimenko.** 2003. Methanogenic sarcina from an anaerobic microbial community degrading *p*-toluene sulfonate. Microbiology **72:**490–495.
45. **Sogin, M. L., and J. H. Gunderson.** 1997. Structural diversity of eukaryotic small subunit ribosomal RNAs. Ann. N. Y. Acad. Sci. **503:**125–139.
46. **Sokal, R. R., and C. D. Michener.** 1958. A statistical method for evaluating systematic relationships. Univ. Kansas Sci. Bull. **28:**1409–1438.
47. **Stackebrandt, E., and F. A. Rainey.** 1995. Partial and complete 16S rDNA sequences, their use in generation of 16S rDNA phylogenetic trees and their implications in molecular ecological studies, chapter 3.1.1, p. 1–17. *In* A. D. L. Akkermans, J. D. van Elsas, and F. J. de Bruijn (ed.), Molecular microbial ecology manual. Kluwer Academic Publishers, Dordrecht, The Netherlands.
48. **Takishita, K., H. Miyake, M. Kawato, and T. Maruyama.** 2005. Genetic diversity of microbial eukaryotes in anoxic sediment around fumaroles on a submarine caldera floor based on the small-subunit rDNA phylogeny. Extremophiles **9:**185–196.
49. **Thomsen, T. R., K. Finster, and N. B. Ramsing.** 2001. Biogeochemical and molecular signatures of anaerobic methane oxidation in a marine sediment. Appl. Environ. Microbiol. **67:**1646–1656.
50. **van der Maarel, M. J. E. C., and T. A. Hansen.** 1997. Dimethylsulfoniopropionate in anoxic intertidal sediments: a precursor of methanogenesis via dimethyl sulfide, methanethiol, and methiolpropionate. Mar. Geol. **137:**5–12.
51. **Vetriani, C., H. W. Jannasch, B. J. MacGregor, D. A. Stahl, and A. L. Reysenbach.** 1999. Population structure and phylogenetic characterization of marine benthic *Archaea* in deep-sea sediments. Appl. Environ. Microbiol. **65:**4375–4384.
52. **Volkman, J. K., D. Rohjans, J. Rullkötter, B. M. Scholz-Böttcher, and G. Liebezeit.** 2000. Sources and diagenesis of organic matter in tidal flat sediments from the German Wadden Sea. Continental Shelf Res. **20:**1139–1158.
53. **von Wintzingerode, F., U. B. Göbel, and E. Stackebrandt.** 1997. Determination of microbial diversity in environmental samples: pitfalls of PCR-based rRNA analysis. FEMS Microbiol. Rev. **21:**213–229.
54. **Webster, G., R. J. Parkes, J. C. Fry, and A. J. Weightman.** 2004. Widespread occurrence of a novel division of bacteria identified by 16S rRNA gene sequences originally found in deep marine sediments. Appl. Environ. Microbiol. **70:**5708–5713.
55. **Whitman, W. B., D. C. Coleman, and W. J. Wiebe.** 1998. Prokaryotes: the unseen majority. Proc. Natl. Acad. Sci. USA **95:**6578–6583.
56. **Wilms, R., B. Köpke, H. Sass, T. S. Chang, H. Cypionka, and B. Engelen.** 2006. Deep biosphere-related bacteria within the subsurface of tidal flat sediments. Environ. Microbiol. **8:**709–719.